Two-qubit separabilities as piecewise continuous functions of maximal concurrence

2008 J. Phys. A: Math. Theor. 41 505303

(http://iopscience.iop.org/1751-8121/41/50/505303)

IOP PUBLISHING JOURNAL OF PHYSICS A: MATHEMATICAL AND THEORETICAL

J. Phys. A: Math. Theor. **41** (2008) 505303 (9pp) doi:10.1088/1751-8113/41/50/505303

Two-qubit separabilities as piecewise continuous functions of maximal concurrence

Paul B Slater

ISBER, University of California, Santa Barbara, CA 93106, USA

E-mail: slater@kitp.ucsb.edu

Received 28 August 2008, in final form 9 October 2008
Published 10 November 2008
Online at stacks.iop.org/JPhysA/41/505303

Abstract

The generic real ($\beta = 1$) and complex ($\beta = 2$) two-qubit states are 9-dimensional and 15-dimensional in nature, respectively. The *total* volumes of the spaces they occupy with respect to the Hilbert–Schmidt and Bures metrics are obtainable as special cases of formulae of Życzkowski and Sommers. We claim that if one could determine certain metric-*independent* three-dimensional '*eigenvalue*-parameterized separability functions' (EPSFs), $S_4^{(1,\beta)}(\lambda_1 \ldots \lambda_4)$, then these formulae could be readily modified so as to yield the Hilbert–Schmidt and Bures volumes occupied by only the *separable* two-qubit states (and hence associated separability *probabilities*). Motivated by analogous earlier analyses of '*diagonal-entry*-parameterized separability functions', we further explore the possibility that such three-dimensional EPSFs might, in turn, be expressible as *univariate* functions of some special relevant variable—which we hypothesize to be the maximal *concurrence* ($0 \leqslant C \leqslant 1$) over spectral orbits. Extensive numerical results that we obtain are rather closely supportive of this hypothesis. *Both* the real and complex estimated EPSFs exhibit clearly pronounced *jumps* of magnitude roughly 50% at $C = \frac{1}{2}$, as well as a number of additional *matching* discontinuities.

PACS numbers: 03.67.−a, 02.30.Cj, 02.40.Ky, 02.40.Ft
Mathematics Subject Classification: 81P05, 52A38, 15A90, 28A75

(Some figures in this article are in colour only in the electronic version)

1. Introduction

In a pair of major, skillful papers, using concepts of random matrix theory, Życzkowski and Sommers were able to obtain exact formulae for the *total* volumes—both in terms of the Hilbert–Schmidt (HS) metric [1] and Bures (minimal monotone) metric [2]—of the $(N^2 - 1)$-dimensional convex set of $N \times N$ complex density matrices and the $((N^2 + N - 2)/2)$-dimensional convex set of $N \times N$ real density matrices, representing N-level quantum

systems (cf [3], [4 sections 14.3, 14.4]). In two recent studies, we have been interested in the question of how to modify/truncate, in some natural manner (by multiplying certain integrands by relevant functions), these formulae of Życzkowski and Sommers, so that they will yield not total volumes, but only the (lesser, strictly included) volumes occupied by the *separable/nonentangled* states [5, 6] (cf [7]). We will report below some interesting progress in this regard, in relation to the two-qubit ($N = 4$) states.

To begin, we present two parallel formulae from [1, 2] for certain generalized normalization constants $\left(C_N^{(\alpha,\beta)}\right)$ used in the total HS and Bures volume computations. (Some notation and formatting has been altered.) For the HS case, we have [1, equation (4.1)] (cf [4, equation (14.35)])

$$\frac{1}{C_{N(HS)}^{(\alpha,\beta)}} = \int_0^\infty \prod_{i=1}^N \mathrm{d}\lambda_i \delta\left(\sum_{i=1}^N \lambda_i - 1\right) \prod_{i=1}^N \lambda_i^{\alpha-1} \prod_{i<j} |\lambda_i - \lambda_j|^\beta, \tag{1}$$

and for the Bures case [2, equation (3.19)] (cf [4, equation (14.46)]),

$$\frac{1}{C_{N(Bures)}^{(\alpha,\beta)}} = \int_0^\infty \prod_{i=1}^N \frac{\mathrm{d}\lambda_i}{\lambda_i^{1/2}} \delta\left(\sum_{i=1}^N \lambda_i - 1\right) \left[\prod_{i<j}^{1\ldots N} \frac{(\lambda_i - \lambda_j)^2}{\lambda_i + \lambda_j}\right]^{\beta/2} \prod_{i=1}^N \lambda_i^{\alpha-1}. \tag{2}$$

The λ's are the N (nonnegative) eigenvalues—constrained to sum to 1—of the corresponding $N \times N$ density matrices, while the parameter β is a 'Dyson index', with $\beta = 1$ corresponding to the real case, and $\beta = 2$, the complex case (and $\beta = 4$, the quaternionic case, not explicitly discussed in [1, 2]). The parameter α will be equal to 1 for the case—of immediate interest to us here—of generically *nondegenerate* density matrices.

1.1. Objective

Our goal, in overall terms, is to find metric-*independent* (separability) functions,

$$S_N^{(\alpha,\beta)}(\lambda_1 \ldots \lambda_N), \tag{3}$$

which, if inserted into formulae (1) and (2) under the integral signs, as simple multiplicative factors, will yield separable—rather than total—volumes when the resulting modified $C_N^{\alpha,\beta}$'s are employed in exactly the same auxiliary computations (involving flag manifolds) in [1] and [2] as the $C_N^{\alpha,\beta}$'s given by (1) and (2) were there. More specifically here, our numerical analyses will be restricted to the $N = 4$ and $\beta = 2$ (complex), and $\beta = 1$ (real) cases.

Our metric-independent goal is plausible for the following reason. Precisely the same preliminary integrations—respecting the separability constraints—over the non-eigenvalue parameters (possibly, Euler angles [8], [6, appendix I]) must be performed for both metrics before arriving at the stage at which we must concern ourselves with the remaining integration over the eigenvalues and the *differences* that are now clearly apparent between metrics in their corresponding measures over the simplex of eigenvalues. Although we are not able to explicitly/symbolically determine what the results of these preliminary integrations might be (the computational challenges are certainly considerable), they must—whatever form they may take—obviously be the same for both metrics in question. Our goal here is to understand—with the assistance of numerical methods—what functional forms these preliminary (12-dimensional in the complex case and 9-dimensional in the real case) integrations yield.

1.2. Maximal concurrence and absolute separability

The further narrower specific focus of this study will be to explore the possibility that there exists a functional relationship of the form,

$$S_4^{(1,\beta)}(\lambda_1 \dots \lambda_4) = \sigma^{(\beta)}(C(\lambda_1 \dots \lambda_4)), \tag{4}$$

where $\sigma^{(\beta)}(x)$ are some unknown *univariate* (*one*-dimensional) functions and

$$C(\lambda_1 \dots \lambda_4) = \max\{0, \lambda_1 - \lambda_3 - 2\sqrt{\lambda_2 \lambda_4}\}, \qquad \lambda_1 \geqslant \lambda_2 \geqslant \lambda_3 \geqslant \lambda_4 \tag{5}$$

is the *maximal concurrence* over spectral orbits of two-qubit density matrices [9, section VII] [10, 11].

For two-qubit states, $C \in [0, 1]$, with $C = 0$ corresponding to the *absolutely* separable states. That is, *no* density matrix with $C = 0$ can be nonseparable/entangled [12]. (In a recent study, we were able to obtain *exact* expressions—involving the tetrahedral dihedral angle $\cos^{-1}\left(\frac{1}{3}\right)$—for the contributions to the Hilbert–Schmidt real and complex two-qubit volumes for those states with $C = 0$, and to numerically estimate the Bures counterparts [6, sections III.B, III.C]. In numerical terms, the HS *absolute* separability probability of generic complex two-qubit states is 0.003 658 26, and the Bures counterpart is 0.000 161 792. The HS real analogue is 0.034 8338.) The *concurrence* itself is a widely used entanglement measure of bipartite mixed states [4, equation (15.26)].

1.3. Motivation

Certainly part of our motivation for advancing the ansatz (4) was that an analogous modeling of a *trivariate* function in terms of a *univariate* function was found to hold—making use of the Bloore (correlation coefficient) parameterization of density matrices [13]—for *diagonal-entry*-parameterized separability functions [14, equation (6)] [15]. This led to substantial insights—and *exact* conjectures $\left(\frac{8}{33}\right.$ and $\left.\frac{8}{17}\right)$—with regard to Hilbert–Schmidt (complex and real) two-qubit separability probabilities. (The Dyson indices β played a central analytical role there, in relating real and complex (and quaternionic) results, but not apparently—as far as we can perceive—in the analyses to be presented below.)

2. Numerics

2.1. Methodology

We do find encouragement in advancing the ansatz (4) by the extensive numerical results we generate, in that our estimates of $\sigma^{(1)}(C)$ and $\sigma^{(2)}(C)$ shown in figure 1 rather closely reproduce—as we will indicate below (section 2.2)—other (independent) numerical results and accompanying conjectures that we have previously obtained.

The $\beta = 2$ complex curve shown in figure 1 is based on the use for quasi-Monte Carlo numerical integration of 26 300 000 12-dimensional (Tezuka–Faure (TF) [16]) *low-discrepancy* points, and the $\beta = 1$ case, on 33 000 000 six-dimensional such points. (The TF procedure—programmed in Mathematica by Giray Ökten [17]—is not conducive to the placing of error bars on the results, though later routines developed by him are.) These points comprise *sample* values, respectively, of the 12 Euler angles used to parameterize $SU(4)$ and the 6 Euler angles used for $SO(4)$. For *each* TF-point, 499 auxiliary computations were carried out—in addition to that of the corresponding Haar measure associated with the Euler angles—for sets of eigenvalues with values of maximal concurrence running at equally spaced intervals from $\frac{1}{500}$ to $\frac{499}{500}$.

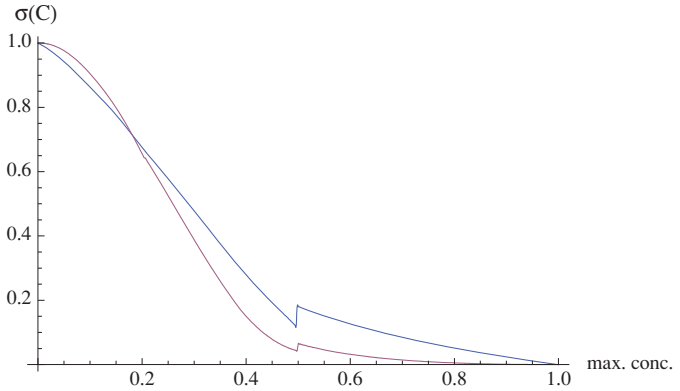

Figure 1. Joint plot of estimated (real (blue, $\beta = 1$) and complex (red, $\beta = 2$)) functions of the maximal concurrence over spectral orbits, $S_4^{(1,\beta)}(\lambda_1 \ldots \lambda_4) = \sigma^{(\beta)}(C(\lambda \ldots \lambda_4))$. Note evident jumps in both functions when the maximal concurrence equals 0.5. The graphs cross at $C = 0.181\,245$ (below which point the complex curve is the greater of the two). For $C = 0, \sigma(C) = 1$, so all associated density matrices are separable.

Each density matrix generated—corresponding to a specific set of eigenvalues with fixed C and Euler angles [8] [6, appendix I]—was tested for separability. Prior to the quasi-Monte Carlo runs, we established a database—using the Mathematica command 'FindInstance'—of 100 sets of four eigenvalues for each of the equally spaced 499 values of C. One of the 100 sets was randomly selected (and then randomly permuted) for each of the TF-points and each of the 499 iterations. This 'random generation' of sets of eigenvalues with *fixed* values of C is clearly less than an ideal procedure, but it was what we found to be practical under the particular circumstances. (In section 2.5, we manage to improve upon this approach.)

Several weeks of MacMini computer time were used for each of the two sets—real and complex—of calculations. (Along with the computations concerning the maximal concurrence (5), we also carried out a fully parallel set of computations using the related variable, $\frac{2\sqrt{\lambda_2\lambda_4}}{\lambda_1-\lambda_3}$. Those results, however, seemed comparatively disappointing in their predictive power, so we do not detail them here.)

2.2. *Evaluation of numerical results*

Let us now appraise our estimated functions (figure 1) by seeing how well they are able to reproduce previous related results, themselves based on very extensive analyses (mostly involving quasi-Monte Carlo integration also).

2.2.1. Complex case. Use of the complex ($\beta = 2$) function in figure 1 impressively explains 98.7253% of the variance of the estimated trivariate eigenvalue-parameterized separability function for $C > 0$ presented in [5, section III.B]. It also yields an estimate of 0.254 756 for the Hilbert–Schmidt separability probability, while our exact conjecture from [15] is $\frac{8}{33} \approx 0.242\,424$. Further, the Bures separability probability estimate yielded is 0.069 2753, while our conjectured value is $\frac{1680(-1+\sqrt{2})}{\pi^8} \approx 0.073\,3389$ [18].

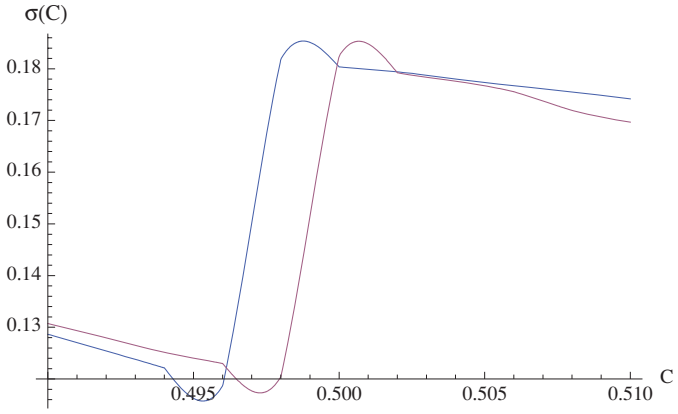

Figure 2. Same plot as figure 1, restricted to the vicinity of $C = \frac{1}{2}$, and the complex (red, 'delayed') curve being amplified by a factor of 2.8.

2.2.2. Real case. Passing to the real ($\beta = 1$) case, we had previously formulated the conjecture that the HS separability probability is $\frac{8}{17} \approx 0.470\,588$ [15, section 9.1]. Our estimate based on the (blue) function shown in figure 1 is 0.480 302. (The corresponding estimate—for which we have no prior conjecture—for the Bures *real* two-qubit separability probability is 0.212 152.) Further, we are able to reproduce 97.7502% of the variation in the corresponding trivariate function for $C > 0$. (This last function had been estimated using a recent Euler-angle parameterization of $SO(4)$, obtained by Cacciatori [6, appendix I]. It was derived by Cacciatori after the submission of [5], and thus not reported or used there, although its complex counterpart—based on 3600 000 Tezuka–Faure points—had been [5, section III.B], while the real case was based on a considerably lesser number of TF-points, 700 000.)

2.3. Jumps near $C = \frac{1}{2}$

For the real ($\beta = 1$) case, the jump near $C(\lambda_1 \ldots \lambda_4) = \frac{1}{2}$ is from approximately 0.118 696 to 0.180 357, and in the complex ($\beta = 2$) case, from 0.0439 255 to 0.651 586. The magnitudes of the two jumps are then quite comparable, being respectively 51.964% and 51.488%. In figure 2, we replot the curves shown in figure 1 in the immediate vicinity of $C = \frac{1}{2}$, but amplify the complex (red) curve by a factor of 2.8. We perceive a very close similarity in shape.

2.4. Additional discontinuities

In figure 3 we show the *derivatives* with respect to C of the estimates of $\sigma^{(\beta)}(C)$. (Figure 4 is a plot of the same two curves, except that we have now added 10 to the derivative in the real case and subtracted 10 in the complex case, so that the discontinuities can be more readily distinguished and compared.) In addition to the already-discussed behavior at $C = 1/2$, we see—*both* in the real and complex cases—a secondary spike at $\frac{147}{500} = 0.294$, and lesser spikes at $\frac{51}{250} = 0.204$ and $\frac{17}{50} = \frac{51}{150} = 0.34$. So, all the observed spikes, signaling what we presume are discontinuities in the $\sigma^{(\beta)}$'s, and concomitant nontrivial *piecewise* behavior—indicative of different separability constraints becoming active/binding or not—are for $C \leqslant \frac{1}{2}$. The

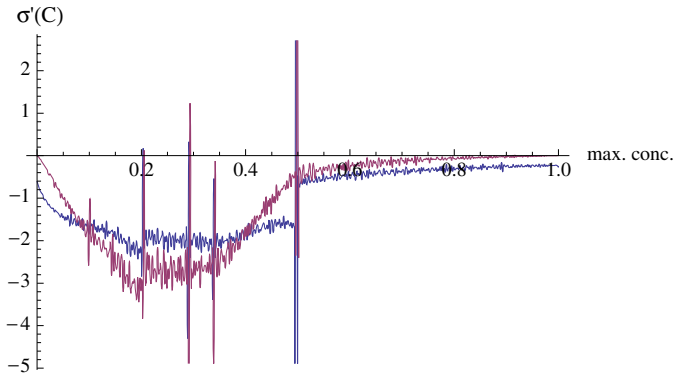

Figure 3. Joint plot of *derivatives* with respect to C of the estimated (real (blue, $\beta = 1$) and complex (red, $\beta = 2$)) functions of the maximal concurrence over spectral orbits $\sigma^{(\beta)}(C(\lambda \ldots \lambda_4))$. Spikes are observable—*both* for the real and complex cases—at $\frac{1}{2} = 0.5$, $\frac{147}{500} = 0.294$, $\frac{51}{250} = 0.204$ and $\frac{17}{50} = \frac{51}{150} = 0.34$.

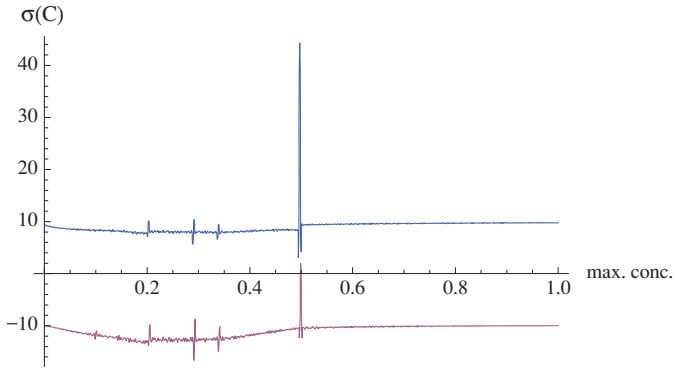

Figure 4. Same as figure 3, except that the real (blue) curve has been translated upwards by 10 units and the complex (red) curve downwards by 10 units, so that the individual discontinuities in the two derivatives can be more readily seen and compared.

point $C = \frac{51}{500} = 0.102$ may also be a discontinuity, at least in the complex case. We could detect no apparent spikes/discontinuities in the upper half-range, $C \in \left[\frac{1}{2}, 1\right]$. (In a somewhat analogous study of two-qubit *three*-parameter HS separability *probabilities*, intricate *piecewise* continuous behavior (involving the *golden ratio*) was observed [19, equation (37) and figure 11].)

In figure 5, we show the segments of the estimated functions $\sigma^{(\beta)}(C)$ between the two discontinuities, $\frac{51}{250} = 0.204$ and $\frac{17}{50} = 0.34$. The behavior seems very close to *linear* for both curves, except for the intermediate discontinuity at $\frac{147}{500} = 0.294$.

2.5. Supplementary analyses

Since the completion of the extensive numerical analyses described above, we have undertaken supplementary, parallel analyses in which 5000 (rather than 500) subintervals of $C \in [0, 1]$ are employed, as well as an improved method is used for sampling random eigenvalues with fixed values of C (using the Mathematica FindInstance command, now with a random seed).

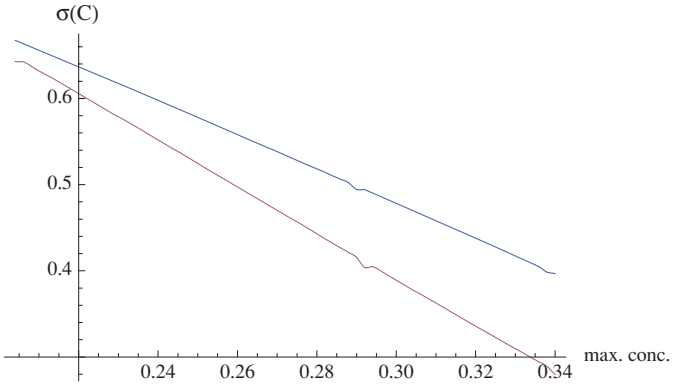

Figure 5. Joint plot of estimated (real (blue, $\beta = 1$) and complex (red, $\beta = 2$)) functions of the maximal concurrence over spectral orbits, $S_4^{(1,\beta)}(\lambda_1 \ldots \lambda_4) = \sigma^{(\beta)}(C(\lambda \ldots \lambda_4))$. The graphs are obviously close to linear between the discontinuities $\frac{51}{250} = 0.204$ and $\frac{17}{50} = 0.34$, except for the intermediate discontinuity at $\frac{147}{500} = 0.294$. To high accuracy, the real (blue) curve can be fitted by the line $1.076\,14 - 1.994\,72C$ and the complex (red, more steeply downward-sloping) curve by $1.198\,22 - 2.695\,48C$.

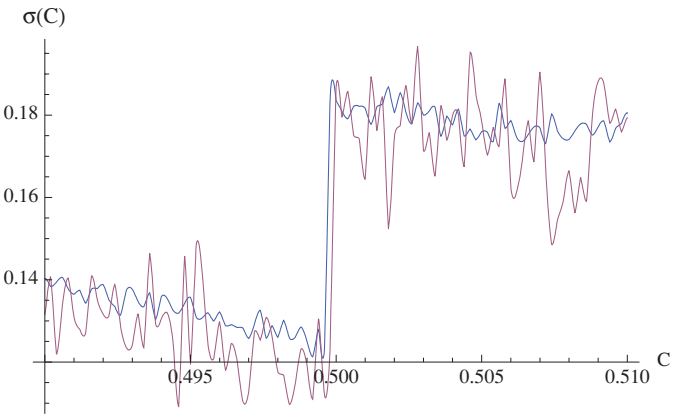

Figure 6. The same plot as figure 2, but based on our ongoing supplementary analysis with finer resolution in C and enhanced eigenvalue sampling. The twin jumps in the estimated eigenvalue-parameterized real and complex separability functions near $C = \frac{1}{2}$ are now certainly indisputably clear. (The complex curve is the more erratic one.)

These results so far seem largely consistent with those already described. However, the new analogues of the plots of derivatives figures 3 and 4, are still much too rough in character to detect the presence of any secondary (non-jump) discontinuities. But, even at this stage (having tested 30 400 times the separability of 4999 complex density matrices and 28 100 times the separability of 4999 real density matrices), we can produce the interesting counterpart (figure 6) to figure 2, in which the two jumps near $C = \frac{1}{2}$ of roughly 50% magnitude are clearly unmistakable. Further, the highly linear behavior displayed in figure 5 also reappears (figure 7).

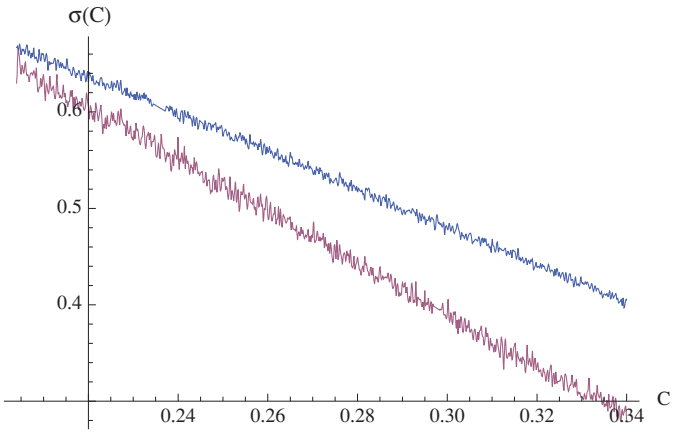

Figure 7. Same plot as figure 5, but based on our ongoing supplementary analysis with finer resolution in C and enhanced eigenvalue sampling.

3. Concluding remarks

For the real and complex two-qubit systems, we have investigated the possibility that the associated (*three*-dimensional) *eigenvalue*-parameterized separability functions—conceptually important for computing separability *probabilities*—are expressible as *one*-dimensional functions ($\sigma(C)$) of the maximal concurrence over spectral orbits ($C \in [0, 1]$). Our numerical estimates, in this regard, have been encouraging, in that they closely reproduce *independently* generated numerical results and exact conjectures concerning separability probabilities based on the Hilbert–Schmidt and Bures (minimal monotone) metrics over the two-qubit systems, and based on the use of *diagonal-entry*-parameterized separability functions. Plots of the real and complex versions of $\sigma(C)$ *both* exhibit *jumps* of approximately 50% magnitude near the midpoint, $C = \frac{1}{2}$, and *both* also indicate the presence of, at least, three further (non-jump) discontinuities ($C \approx 0.204, 0.294, 0.34$), apparently indicative of points at which certain distinct separability constraints become either active/binding or not. Over the interval $C \in [0.204, 0.34]$, the real and complex fitted functions $\sigma(C)$ *both* appear to be simply linear (except at $C \approx 0.294$).

We have principally studied above the possibility (4) that the ostensibly *trivariate* two-qubit eigenvalue-separability functions can be equivalently expressed as *univariate* functions of only a single variable, that is, the maximal concurrence C over spectral orbits [9]. Since we have unfortunately not been able to fully formally resolve this issue—although our supporting evidence for this proposition is intriguing—we cannot also presently fully eliminate the possibility that one or even two (yet unspecified) variables supplemental to C are in fact needed, and that the corresponding separability function is not in fact strictly univariate in nature (as we do know it definitely is the case with the two-qubit diagonal-entry-parameterized separability functions [15]).

It presently appears somewhat problematical to extend the line of analysis above to the qubit–*qutrit* ($N = 6$) case. In addition, to simply the greatly increased computational burden that would be involved, there does not seem to be a maximal concurrence formula comparable to the two-qubit one (5) with the requisite properties we have utilized [9, pp 102108–16].

We have examined the relationship between separability and entanglement in a specific analytical setting—involving *eigenvalue*-parameterized separability functions and the use of the Życzkowski–Sommers formulae [1, 2] for the total Hilbert–Schmidt and Bures volumes of the $N \times N$ density matrices. A number of studies of Batle, Casas, Plastino and Plastino (for example, [20]) have also focused on the relationship between separability and entanglement, but in somewhat different analytical frameworks (typically involving the ZHSL measure [7], which is *uniform* over the eigenvalue simplex). The closest we can come, it seems, to a direct comparison with their analyses is to note that the dot-dashed curve in figure 2 of [20] is based on the Hilbert–Schmidt metric, and their x-axis is the Bures distance, while we have employed the maximal concurrence C on the x-axis in the somewhat comparable figure 1 above (cf [21]). Both theirs and our plots are, in general, downward decreasing, but theirs gives no indication of any discontinuities. Also, their plot is of the separability *probability*, while ours is of the (presumed univariate) eigenvalue-parameterized separability *function*, to be used in the computation of the probability.

Acknowledgments

I would like to express appreciation to the Kavli Institute for Theoretical Physics (KITP) for computational support in this research.

References

[1] Życzkowski K and Sommers H-J 2003 *J. Phys. A: Math. Gen.* **36** 10115
[2] Sommers H-J and Życzkowski K 2003 *J. Phys. A: Math. Gen.* **36** 10083
[3] Andai A 2006 *J. Phys. A: Math. Gen.* **39** 13641
[4] Bengtsson I and Życzkowski K 2006 *Geometry of Quantum States* (Cambridge: Cambridge University Press)
[5] Slater P B 2008 *J. Geom. Phys.* **58** 1101
[6] Slater P B 2008 (doi:10.1016/j.geomphys.2008.08.008)
[7] Życzkowski K, Horodecki P, Sanpera A and Lewenstein M 1998 *Phys. Rev.* A **58** 883
[8] Tilma T, Byrd M and Sudarshan E C G 2002 *J. Phys. A: Math. Gen.* **35** 10445
[9] Hildebrand R 2007 *J. Math. Phys.* **48** 102108
[10] Ishizaka S and Hiroshima T 2000 *Phys. Rev.* A **62** 022310
[11] Verstraete F, Audenaert K and Moor B D 2001 *Phys. Rev.* A **64** 012316
[12] Wootters W K 1998 *Phys. Rev. Lett.* **80** 2245
[13] Bloore F J 1976 *J. Phys. A: Math. Gen.* **9** 2059
[14] Slater P B 2007 *Phys. Rev.* A **75** 032326
[15] Slater P B 2007 *J. Phys. A: Math. Gen.* **40** 14279
[16] Faure H and Tezuka S 2002 *Monte Carlo and Quasi-Monte Carlo Methods 2000 (Hong Kong)* ed K T Tang, F J Hickernell and H Niederreiter (Berlin: Springer) p 242
[17] Ökten G 1999 *MATHEMATICA in Educ. Res.* **8** 52
[18] Slater P B 2005 *J. Geom. Phys.* **53** 74
[19] Slater P B 2006 *J. Phys. A: Math. Gen.* **39** 913
[20] Batle J, Casas M, Plastino A and Plastino A R 2006 *Phys. Lett.* A **353** 161
[21] Batle J, Plastino A R, Casas M and Plastino A 2002 *Phys. Lett.* A **298** 301